Molecular Biology Reports (2026) 53:1898
https://doi.org/10.1007/s11033-026-13052-7

ORIGINAL ARTICLE

Gossypetin and luteolin, alone and with cisplatin, preferentially reduce MCF-7 breast cancer cell viability, whereas HeLa cervical cancer cells are refractory

Elif Candan[1] · **Zeynep Ülker**[2]

Received: 16 July 2026 / Accepted: 20 October 2026
© The Author(s), under exclusive licence to Springer Nature B.V. 2026

Abstract

Background Dietary flavonoids have been proposed as partners for platinum chemotherapy, but their effects vary between tumour types, and sparing of normal cells has to be demonstrated. We examined gossypetin and luteolin, alone and combined with cisplatin, in MCF-7 breast and HeLa cervical carcinoma cells and in non-tumorigenic L929 fibroblasts.

Methods and Results Cells were exposed to 100 µg/mL cisplatin (CP), gossypetin (GOS), luteolin (LUT) or their double and triple combinations. Viability was measured by MTT assay (technical triplicates, one experiment), combination effects by Bliss independence, Bax, Bcl-2 and CASP3 transcripts by RT-PCR ($2^{-\Delta\Delta Ct}$), and phosphatidylserine exposure by Annexin V–Cy3 staining of archived micrographs. At 48 h, six of the seven treatments reduced MCF-7 viability (61.8–85.0% of control; Tukey-adjusted $p \leq 0.018$), gossypetin being the most active. Cisplatin plus luteolin exceeded the Bliss expectation in MCF-7 at 24 h (excess + 0.11), whereas all combinations were less than additive at 48 h. No treatment reduced HeLa viability, and HeLa cells showed Bcl-2 induction (1.9–30.2-fold) with Bax repression (Bax/Bcl-2 ratio 0.03–0.21). L929 viability was not reduced at either time point, and the archived L929 field showed no Annexin V labelling.

Conclusions At this single concentration, gossypetin- and luteolin-based treatments reduced MCF-7 viability without reducing L929 viability, while HeLa cells were refractory at the viability and transcript levels. These retrospective data support dose–response and protein-level studies rather than mechanistic conclusions.

✉ Zeynep Ülker
zeynep.ulker@galata.edu.tr

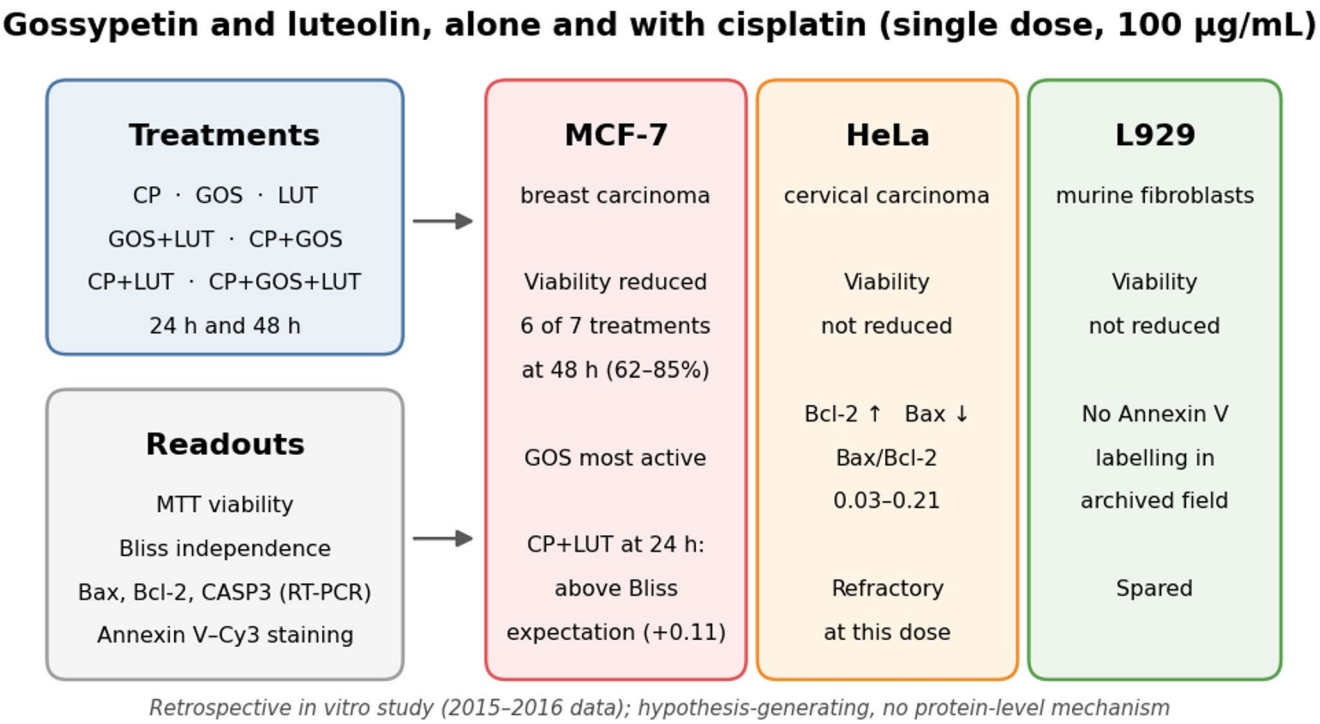
Elif Candan
elf.candan@gmail.com

[1] Istanbul University, Istanbul, Türkiye

[2] Department of Basic Sciences, Faculty of Dentistry, Istanbul Galata University, Istanbul, Türkiye

Published online: 04 November 2026

Graphical Abstract



Keywords Gossypetin · Luteolin · Cisplatin · Breast cancer · Bax/Bcl-2 · Drug combination

Introduction

Breast cancer is the most frequently diagnosed cancer in women, and cervical cancer remains a leading cause of cancer death in low-resource settings [1]. Cisplatin is still widely used against both diseases. It forms DNA adducts that block replication and trigger apoptosis [2, 3], but its clinical benefit is limited by nephrotoxicity, ototoxicity and myelosuppression, and by acquired resistance through enhanced DNA repair, reduced drug accumulation and evasion of apoptosis [4]. Combining cisplatin with natural compounds that increase tumour-cell killing without adding toxicity has therefore been explored in several tumour models [5–8].

Resistance to apoptosis is central to this problem. Many tumours over-express anti-apoptotic members of the Bcl-2 family, which raises the threshold for mitochondrial cell death and weakens the response to chemotherapy [9]. The intrinsic pathway is controlled by the balance between pro-apoptotic proteins such as Bax and anti-apoptotic proteins such as Bcl-2. When Bax prevails, the mitochondrial outer membrane is permeabilised, cytochrome c is released and caspases are activated [10, 11]. For this reason the Bax/Bcl-2 ratio is often used as a readout of apoptotic potential [12].

Flavonoids are dietary polyphenols with anti-proliferative and pro-apoptotic activity in many cancer models [13]. Luteolin (3′,4′,5,7-tetrahydroxyflavone) is among the best studied. It induces cell-cycle arrest and apoptosis in breast and cervical carcinoma cells, often through changes in Bcl-2 family proteins and survival kinases [13–16]. It also increases cisplatin sensitivity in ovarian and cervical carcinoma cells [5, 17] and acts synergistically with other agents in cervical cancer cells [18]. Gossypetin (3,5,7,8,3′,4′-hexahydroxyflavone) has received much less attention. It has high radical-scavenging and reducing capacity [19, 20], and anticancer activity has been reported in oral, oesophageal, prostate and skin cancer models, where it affects apoptotic and kinase signalling pathways [21–24]; anti-inflammatory effects have also been described [25]. Its oral pharmacokinetics were characterised only recently [26]. To our knowledge, gossypetin has not been tested in breast or cervical cancer cells or in combination with cisplatin.

In this study we compared the responses of MCF-7 breast and HeLa cervical carcinoma cells and non-tumorigenic L929 fibroblasts to gossypetin and luteolin, alone and with cisplatin, at a single concentration that had been selected to spare L929 cells. We measured viability, combination effects, transcript levels of Bax, Bcl-2 and CASP3, and

phosphatidylserine exposure. The experiments were carried out in 2015–2016, and the present analysis is retrospective.

Materials and methods

Compounds and reagents

Cisplatin, gossypetin and luteolin (analytical grade) were purchased from Sigma-Aldrich (Merck KGaA, Darmstadt, Germany). Gossypetin and luteolin were dissolved in dimethyl sulfoxide (DMSO) and cisplatin in sterile saline. Stock solutions were diluted in culture medium immediately before use to a final concentration of 100 µg/mL for each agent, alone or in combination, and the final DMSO concentration was kept below 0.5% (v/v). This concentration had been chosen in preliminary dose-finding experiments as one that was not cytotoxic to L929 cells, and it was used here as a single test concentration. MTT (3-(4,5-dimethylthiazol-2-yl)-2,5-diphenyltetrazolium bromide) and the Annexin V–Cy3 apoptosis detection kit (BioVision, Milpitas, CA, USA) were used according to the suppliers' instructions.

Cell lines and culture

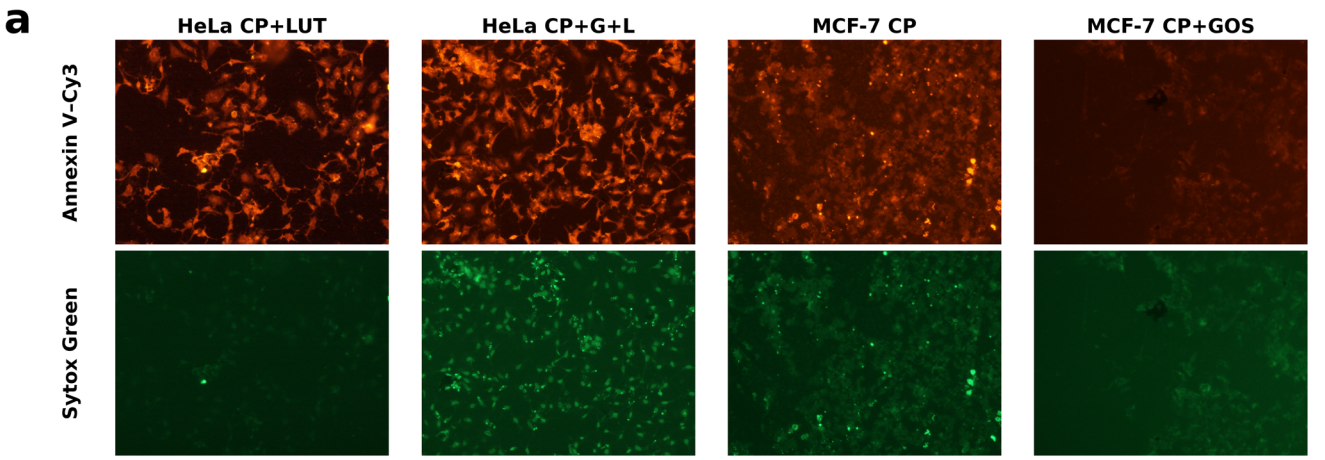
Human breast adenocarcinoma MCF-7 cells (HTB-22), human cervical adenocarcinoma HeLa cells (CCL-2) and murine L929 fibroblasts (CCL-1) were obtained from the American Type Culture Collection (ATCC, Manassas, VA, USA). Cells were grown in Dulbecco's modified Eagle's medium (DMEM) supplemented with 10% fetal bovine serum (FBS; Gibco, Thermo Fisher Scientific, Waltham, MA, USA) and antibiotics at 37 °C in a humidified atmosphere with 5% CO_2, and were passaged with trypsin–EDTA. Cells in exponential growth were used in all experiments. Seeding densities were optimised beforehand by real-time cell analysis (xCELLigence, Roche). L929 cells were included as a non-tumorigenic comparator, as in earlier selectivity studies [27]. Passage numbers were not retained in the archived records.

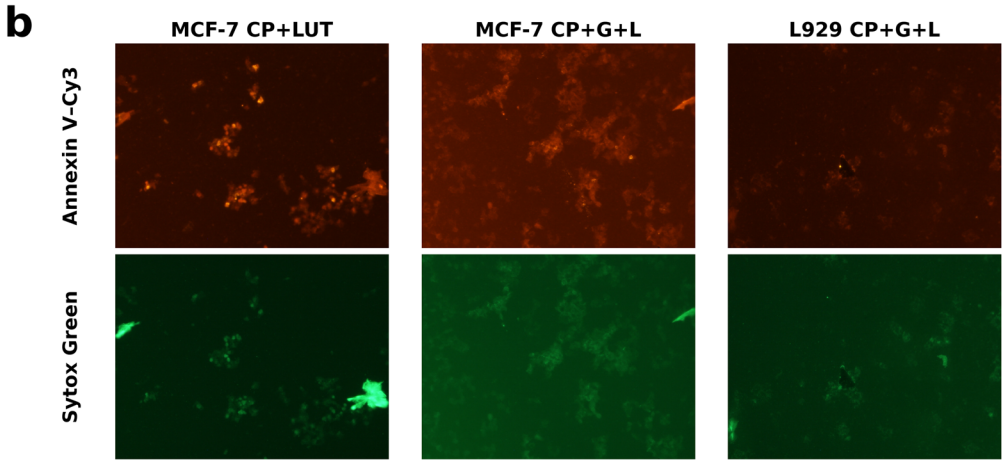
MTT viability assay

Cells were seeded in 96-well plates at 1.5×10^4 cells per well in 100 µL of medium and allowed to attach for 24 h. The medium was then replaced with medium containing the treatments, and untreated wells served as controls. Eight conditions were tested: control, CP, GOS, LUT, GOS + LUT, CP + GOS, CP + LUT and CP + GOS+LUT. After 24–48 h, MTT was added and the plates were incubated for a further 3–4 h at 37 °C. The formazan crystals were dissolved and absorbance was read at 570 nm [28]. Absorbance values were not blank-corrected. Each condition was tested in three wells in one experiment, so the replicates are technical. In this revision all wells were re-extracted from the raw plate records and a single exclusion rule was applied: wells with an optical density below 0.25, which corresponds to cell-free wells, were excluded, and all other wells were retained (Supplementary Table S1). After exclusion, the 48-h L929 control consisted of a single well, and the 48-h L929 data are therefore reported descriptively. The MCF-7 48-h data reported here were obtained in a repeat experiment performed in March 2016 with the same protocol. The corresponding wells of the earlier 48-h experiment could not be identified unambiguously in the archived plate records, so only the repeat experiment is reported. Viability was expressed as a percentage of the mean of the control wells.

Annexin V–Cy3/Sytox Green staining and scoring

Cells were seeded in 96-well plates (1.5×10^4 cells per well), treated for 24 h and washed three times with phosphate-buffered saline (PBS). Each well received 105 µL of staining solution (4 µL Annexin V–Cy3 and 1 µL Sytox Green in 100 µL binding buffer: 10 mM HEPES/NaOH, 140 mM NaCl, 5 mM $CaCl_2$, pH 7.4) and was incubated for 15 min at room temperature in the dark without fixation. After three further washes, cells were imaged on an inverted fluorescence microscope (Leica Microsystems, Wetzlar, Germany) fitted with a ×20 objective, using TRITC (Annexin V–Cy3) and FITC (Sytox Green) filter sets, and fields were recorded with the attached digital camera. The archived image files carry no spatial calibration, so scale bars could not be added retrospectively; the objective magnification is stated in the legend of Fig. 1. Annexin V binding detects phosphatidylserine on the outer leaflet of the plasma membrane, an early feature of apoptosis [29–31]. The original per-field counts were not retained. For this revision, one archived micrograph per condition (640 × 480 pixels) was scored retrospectively for seven conditions. Scoring combined automated threshold-based segmentation, with visual inspection of every mask, and manual counting by quadrant; discrepancies were resolved by consensus, and all counts were checked by the authors. Proportions are given with Wilson 95% confidence intervals where exact counts could be obtained (Supplementary Table S3). No untreated-control field had been archived. On the archived slides, two HeLa channel images had been placed under transposed filter labels, and channel assignment here follows the measured colour content. One archived merge image (MCF-7, CP + LUT) did not correspond to its single-channel images and was excluded.


a
HeLa CP+LUT
HeLa CP+G+L
MCF-7 CP
MCF-7 CP+GOS
Annexin V-Cy3
Sytox Green


b
MCF-7 CP+LUT
MCF-7 CP+G+L
L929 CP+G+L
Annexin V-Cy3
Sytox Green

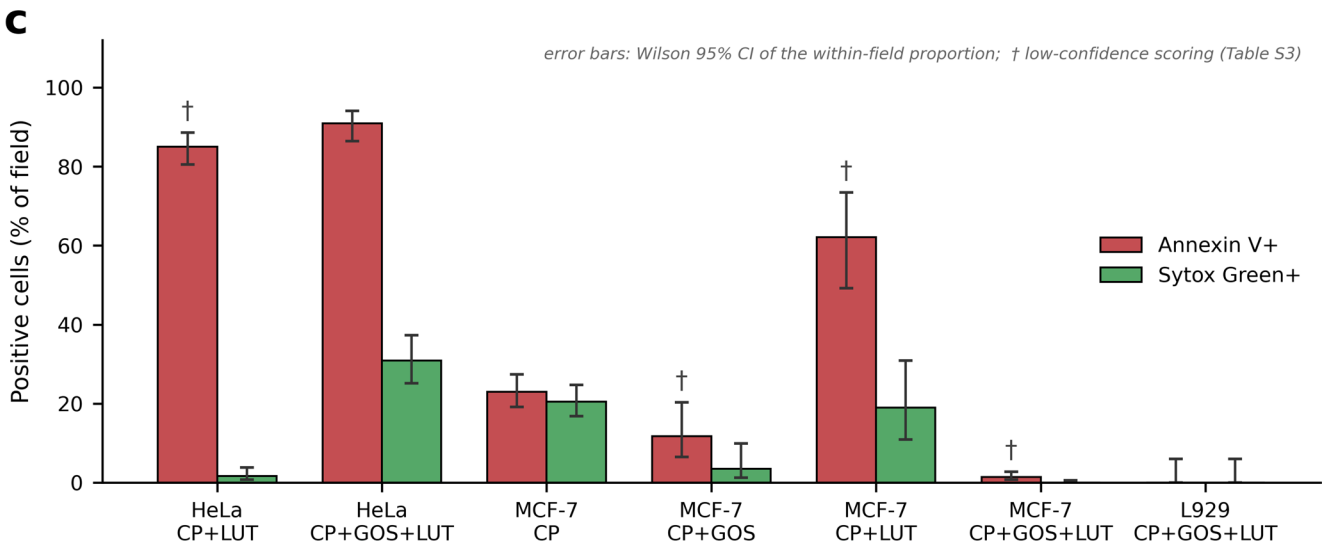

c
error bars: Wilson 95% CI of the within-field proportion; † low-confidence scoring (Table S3)
Positive cells (% of field)
100
80
60
40
20
0
†
Annexin V+
Sytox Green+
HeLa CP+LUT
HeLa CP+GOS+LUT
MCF-7 CP
MCF-7 CP+GOS
MCF-7 CP+LUT
MCF-7 CP+GOS+LUT
L929 CP+GOS+LUT

Fig. 1 Annexin V–Cy3 (red) and Sytox Green (green) staining of archived fields of HeLa, MCF-7 and L929 cells after 24 h treatment with the indicated combinations of cisplatin (CP), gossypetin (G, GOS) and luteolin (L, LUT), with the proportion of Annexin V-positive cells in each field and Wilson 95% confidence intervals where exact counts were available. Each condition is represented by one archived field, acquired with a ×20 objective on an inverted fluorescence microscope (Leica) and shown at its native resolution of 640 × 480 pixels; because the archived files carry no spatial calibration, no scale bar is shown. No untreated-control field was available. Scoring details are given in Supplementary Table S3

RNA isolation and RT-PCR

Total RNA was extracted from treated and control cells and reverse-transcribed to cDNA. Bax, Bcl-2, CASP3 and β-actin transcripts were quantified by real-time PCR in duplicate wells, with one cDNA sample per condition. Primers for the human lines were [32]: Bax, forward 5′-GCCCTTTTGCTTCAGGGTTTC-3′, reverse 5′-TCCAATGTCCAGCCTTTG-3′; Bcl-2, forward 5′-CGGAGGCTGGGATGCCTTTG-3′, reverse 5′-TTTGGGGCAGGCATGTTGAC-3′; β-actin, forward 5′-GAGACCTTCAACACCCCAGCC-3′, reverse 5′-AGACGCAGGATGGCATGGG-3′. Primers for L929 cells were [33]: Bax, forward 5′-GCTTACCGTAGCAGTTGGAT-3′, reverse 5′-GCCTTGAGCACCAGTTTGCT-3′; Bcl-2, forward 5′-ACCCTGTTGTGTAGCCGTCTG-3′, reverse 5′-GCATCCCAGCCTCCGTTATCA-3′. The CASP3 primer records could not be retrieved. Relative expression was calculated by the Livak method as $2^{-\Delta\Delta Ct}$, where $\Delta\Delta Ct = (Ct_{target} - Ct_{\beta-actin})_{treated} - (Ct_{target} - Ct_{\beta-actin})_{control}$, with untreated cells as the calibrator [34]. The mean β-actin Ct varied by 3.0 cycles across conditions in HeLa cells, 3.7 cycles in L929 cells and 13.7 cycles in MCF-7 cells [35]. Because of this instability, MCF-7 transcript data are shown only in Supplementary Fig. S1. During the revision we found that the L929 Bcl-2 Ct values in the archived spreadsheet were identical, well for well, to the HeLa β-actin values, which indicates a transcription error in the original record. L929 Bcl-2 data and L929 Bax/Bcl-2 ratios were therefore excluded.

Combination and statistical analysis

Viability was compared by one-way ANOVA for each cell line and time point, followed by Tukey's test for comparisons with the control. Exact adjusted p values are reported, and "ns" denotes $p \geq 0.05$. Because the replicates are technical wells from one experiment, the p values describe within-plate variation and not reproducibility between experiments. Combination effects were assessed by the Bliss independence model [36, 37]. Fractional inhibition was calculated as $E = 1 - \text{viability}/100$, the expected effect as $E_{exp} = 1 - \Pi(1 - E_{single})$, and the Bliss excess as $E_{obs} - E_{exp}$. Excess values were interpreted only when every single agent in the combination was inhibitory, and values above + 0.10 or below − 0.10 were regarded as synergistic or antagonistic tendencies. Because each agent was tested at one concentration, a dose–response synergy surface could not be constructed. Analyses were performed in Python 3 with SciPy and statsmodels 0.14.

Results

Treatments reduced MCF-7 viability but not HeLa or L929 viability

At 48 h, six of the seven treatments reduced MCF-7 viability relative to the control (Fig. 2; Table 1). Gossypetin was the most active agent (61.8%, $p < 0.001$), followed by CP + GOS (68.5%, $p < 0.001$), GOS + LUT (77.2%, $p < 0.001$), LUT (77.9%, $p < 0.001$), CP + LUT (83.3%, $p = 0.007$) and CP (85.0%, $p = 0.018$). The triple combination did not reach significance (88.9%, $p = 0.12$). At 24 h, CP + LUT (58.5%, $p < 0.001$) and LUT (74.4%, $p < 0.001$) reduced MCF-7 viability, and the other treatments did not.

No treatment reduced HeLa viability at either time point. The only significant change in HeLa cells was an increase with CP + GOS at 48 h (155.8%, $p = 0.004$). L929 viability did not differ from the control at 24 h (ANOVA $p = 0.87$). At 48 h, L929 values ranged from 104% to 199% of a single-well control and were not analysed statistically.

Bliss analysis

Within the range in which the Bliss model could be applied, CP + LUT exceeded the expected effect in MCF-7 cells at 24 h (observed inhibition 0.41, expected 0.31, excess + 0.11) (Supplementary Table S2). At 48 h, all four MCF-7 combinations were less effective than expected (excess − 0.16 to − 0.48). In HeLa cells, CP + LUT at 24 h was additive (excess − 0.07). In all other HeLa and L929 comparisons, at least one single agent was not inhibitory, so the model could not be applied. We therefore do not claim synergy at the concentration tested.

Transcript responses differed between cell lines

In HeLa cells, six of the seven treatments increased Bcl-2 mRNA (1.9–30.2-fold) and all seven decreased Bax mRNA (0.04–0.82-fold), giving Bax/Bcl-2 ratios of 0.03–0.21 (Fig. 3a; Table 2). CASP3 mRNA was at or below the control level except with GOS + LUT (2.5-fold). This profile is consistent with the absence of cytotoxicity in HeLa cells. In L929 cells, Bax mRNA changed in both directions

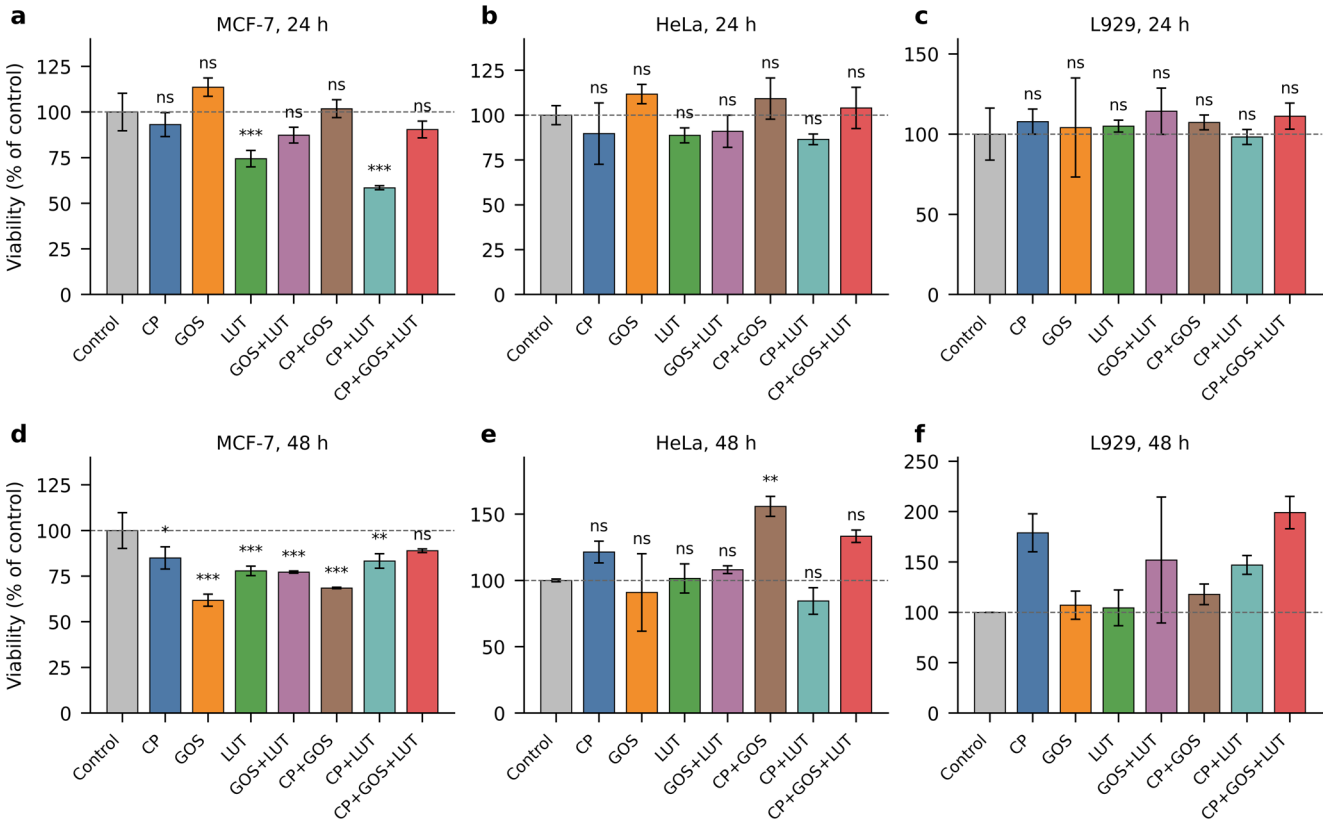


Fig. 2 Viability of MCF-7 (a, d), HeLa (b, e) and L929 (c, f) cells after 24 h (a–c) and 48 h (d–f) exposure to 100 µg/mL cisplatin (CP), gossypetin (GOS), luteolin (LUT) or their combinations, measured by MTT assay. Bars show means ± SD of technical replicate wells from one experiment ($n = 3$, except HeLa 48 h CP + GOS and L929 48 h LUT, $n = 2$). The dashed line marks the untreated control (100%). One-way ANOVA with Tukey's test versus control: * $p < 0.05$, ** $p < 0.01$, *** $p < 0.001$; ns, not significant. Panel f is descriptive only because the 48-h L929 control consisted of one well

Table 1 Cell viability (% of untreated control, mean ± SD) measured by MTT assay after 24 h and 48 h exposure to 100 µg/mL treatments

Treatment	MCF-7 24 h	MCF-7 48 h	HeLa 24 h	HeLa 48 h	L929 24 h	L929 48 h
Control	100.0 ± 10.3	100.0 ± 9.8	100.0 ± 5.3	100.0 ± 1.0	100.0 ± 16.2	100.0 (1)
CP	93.1 ± 6.6 ns	85.0 ± 6.1 *	89.7 ± 17.1 ns	121.4 ± 8.2 ns	107.8 ± 7.8 ns	178.9 ± 18.9
GOS	113.6 ± 5.0 ns	61.8 ± 3.3 ***	111.7 ± 5.4 ns	90.9 ± 29.2 ns	104.1 ± 30.9 ns	107.1 ± 14.0
LUT	74.4 ± 4.5 ***	77.9 ± 2.6 ***	88.7 ± 4.2 ns	101.5 ± 11.0 ns	105.0 ± 3.7 ns	104.4 ± 17.8 (2)
GOS + LUT	87.3 ± 4.3 ns	77.2 ± 0.6 ***	91.0 ± 9.0 ns	108.1 ± 2.9 ns	114.3 ± 14.4 ns	151.9 ± 62.6
CP + GOS	101.8 ± 4.9 ns	68.5 ± 0.4 ***	109.2 ± 11.5 ns	155.8 ± 7.5 (2) **	107.3 ± 4.6 ns	117.8 ± 10.2
CP + LUT	58.5 ± 1.1 ***	83.3 ± 4.0 **	86.5 ± 3.0 ns	84.5 ± 10.0 ns	98.2 ± 4.7 ns	147.0 ± 9.3
CP + GOS + LUT	90.4 ± 4.6 ns	88.9 ± 1.0 ns	104.0 ± 11.5 ns	133.3 ± 4.7 ns	111.2 ± 8.1 ns	199.0 ± 16.0

Values are means ± SD of technical replicate wells from one experiment ($n = 3$ unless shown in parentheses). Wells with OD < 0.25 were excluded (Supplementary Table S1). Tukey-adjusted comparison with control: * $p < 0.05$, ** $p < 0.01$, *** $p < 0.001$; ns, not significant. L929 at 48 h is shown descriptively because the control consisted of one well. MCF-7 48-h data are from the repeat plate of March 2016. CP, cisplatin; GOS, gossypetin; LUT, luteolin

(0.36–2.66-fold) without a consistent pattern, whereas CASP3 mRNA was lower than in the control under all treatments (0.09–0.80-fold) (Fig. 3b). Given the 3.7-cycle variation in the reference gene, we regard these L929 changes as uncertain. MCF-7 transcript data are presented in Supplementary Fig. S1 only.

Annexin V labelling in archived fields

In the archived fields (Fig. 1; Supplementary Table S3), Annexin V–Cy3 membrane labelling was extensive in HeLa cells treated with CP + LUT (approximately 85%, low to moderate confidence) and CP + GOS + LUT (90.9%). In MCF-7 cells, labelling was observed with CP (23.0%), CP + GOS (11.8%) and CP + LUT (62.1%, low confidence),

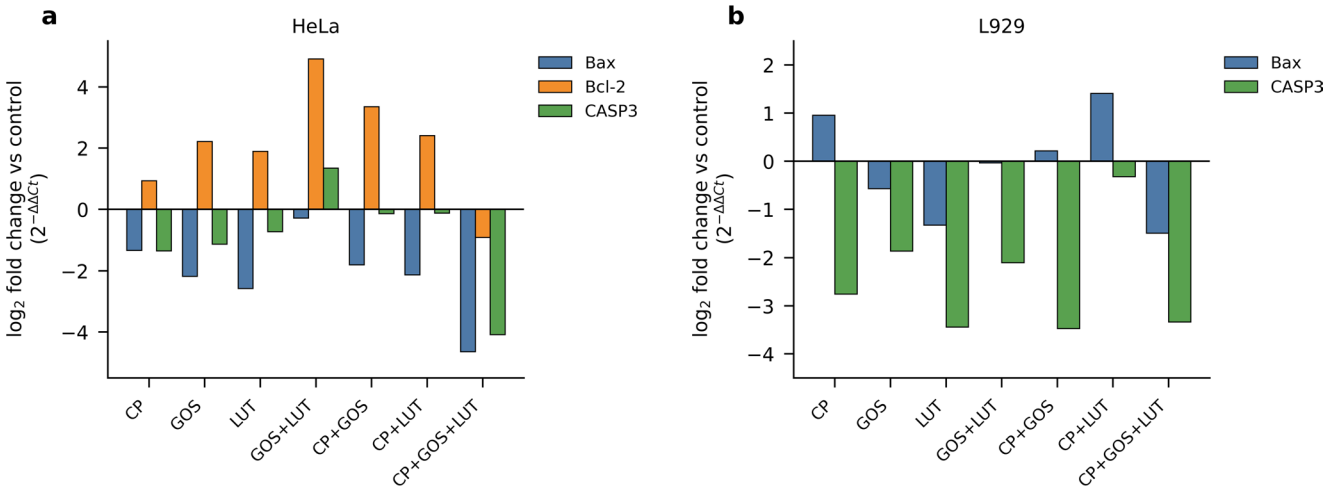


Fig. 3 Relative mRNA levels of Bax, Bcl-2 and CASP3 in HeLa cells (**a**) and of Bax and CASP3 in L929 cells (**b**) after treatment with 100 µg/mL cisplatin (CP), gossypetin (GOS), luteolin (LUT) or their combinations. Values are $\log_2$ fold changes versus untreated control calculated by the $2^{-\Delta\Delta Ct}$ method with β-actin as the reference gene (duplicate PCR wells, one cDNA sample per condition). L929 Bcl-2 is not shown because the archived Ct record was invalid

Table 2 Relative mRNA levels ($2^{-\Delta\Delta Ct}$, fold change versus untreated control) in HeLa and L929 cells

Treatment	HeLa Bax	HeLa Bcl-2	HeLa CASP3	HeLa Bax/Bcl-2	L929 Bax	L929 CASP3
CP	0.39	1.91	0.39	0.206	1.94	0.15
GOS	0.22	4.64	0.45	0.048	0.67	0.27
LUT	0.17	3.72	0.60	0.045	0.40	0.09
GOS + LUT	0.82	30.17	2.54	0.027	0.98	0.23
CP + GOS	0.29	10.23	0.91	0.028	1.16	0.09
CP + LUT	0.23	5.32	0.92	0.043	2.66	0.80
CP + GOS + LUT	0.04	0.53	0.06	0.076	0.35	0.10

β-actin was the reference gene and untreated cells the calibrator (fold change = 1). Values are derived from duplicate PCR wells of one cDNA sample per condition. L929 Bcl-2 data and Bax/Bcl-2 ratios were excluded because of a transcription error in the archived record (see Methods). MCF-7 data are given in Supplementary Fig. S1. CP, cisplatin; GOS, gossypetin; LUT, luteolin

and was almost absent with the triple combination (1–2%). The L929 field treated with the triple combination showed no detectable Annexin V or Sytox Green labelling. Each condition is represented by one field and no control field was available, so these values are qualitative support only.

Discussion

At a single concentration of 100 µg/mL, gossypetin and luteolin, alone and with cisplatin, reduced the viability of MCF-7 cells but not of L929 fibroblasts. Six of seven treatments were active in MCF-7 cells at 48 h, and the only combination that exceeded the Bliss expectation, CP + LUT at 24 h, was also observed in this line. At 48 h the combinations were less than additive, so the combination data do not indicate a consistent benefit over the single agents. Gossypetin alone produced the largest reduction in MCF-7 viability. This is, to our knowledge, the first report of gossypetin activity in breast cancer cells, and it agrees with the growth-inhibitory effects described in other carcinoma models [21–24].

HeLa cells behaved differently. Their viability did not fall, and the transcript response, with Bcl-2 induction and Bax repression, points in the same direction. This pattern is the opposite of the Bax increase and Bcl-2 decrease reported for HeLa cells treated with luteolin [16] and with other flavonoid or natural-product treatments [38, 39], and it is consistent with Bcl-2-mediated evasion of apoptosis as a resistance mechanism [4, 9]. Zhao et al. found that luteolin potentiated cisplatin in HeLa and SiHa cells over a range of concentrations [17]; the single concentration used here may lie outside the effective window for this line. The extensive Annexin V labelling in treated HeLa fields is difficult to reconcile with the viability data. Phosphatidylserine exposure without loss of viability can occur transiently, and diffuse background staining cannot be ruled out in archived fields without controls. We therefore do not interpret this labelling as evidence of apoptosis.

L929 viability was not reduced by any treatment, and the L929 field showed no Annexin V labelling. L929 is one

of the cell lines specified in ISO 10993-5 [40], and it was used by most laboratories in a recent multicentre comparison of cytotoxicity testing [41]; it is also used as a normal-cell comparator in flavonoid studies [42]. HeLa cells were included as a second carcinoma line of female reproductive-tract origin, which allowed us to ask whether the response of MCF-7 cells was shared by another carcinoma type. However, L929 cells are murine fibroblasts and not breast epithelium. A comparison with a non-tumorigenic human breast line such as MCF-10 A would be needed to support breast-specific selectivity [43, 44].

The difference between MCF-7 and HeLa cells is biologically plausible, because sensitivity to flavonoids differs between carcinoma types and combinations of natural compounds with chemotherapeutic drugs give cell-line-dependent results [45, 46]. Our data do not identify the mechanism behind the sensitivity of MCF-7 cells. The transcript assay that could have addressed this question was unreliable in MCF-7 cells, and no protein measurements are available.

Limitations

This is a retrospective analysis of experiments performed in 2015–2016, and we report it so that the data are not lost [47]. Only one concentration was tested, so neither IC_{50} values nor dose–response synergy could be determined. The MTT data come from technical replicates in one experiment, the MCF-7 48-h data come from a repeat plate, and the 48-h L929 control rests on one well. Cisplatin at 100 µg/mL (about 333 µM) was unexpectedly weak in all three lines, which we cannot explain from the records. Flavonoids can reduce MTT directly [48, 49], and no cell-free compound controls or vehicle-control data are available in the analysed dataset, so part of the viability signal in HeLa and L929 cells may reflect assay interference. The transcript data rest on one cDNA sample per condition, the reference gene was unstable, the CASP3 primer records were not retained, and L929 Bcl-2 data had to be excluded. No Western blot, caspase-activity or cytochrome c measurements are available. Annexin V scoring was performed retrospectively on one field per condition without controls. Finally, no non-tumorigenic human breast cell line was included. A prospective study with dose–response designs, independent biological replicates, vehicle and cell-free controls, protein-level markers and MCF-10 A cells is needed to test the observations reported here.

Conclusions

At a single concentration, gossypetin and luteolin, alone and with cisplatin, reduced MCF-7 viability without reducing L929 viability, and CP+LUT showed a synergistic tendency at 24 h. HeLa cells were refractory at both the viability and the transcript level. These retrospective findings justify prospective dose–response and protein-level studies in breast cancer models, but they do not establish a mechanism.

Supplementary Information The online version contains supplementary material available at https://doi.org/10.1007/s11033-026-13052-7.

Author contributions Z.Ü. conceived and supervised the study. E.C. performed the experiments (cell culture, MTT, Annexin V staining, and RT-PCR) and analysed the data. E.C. and Z.Ü. interpreted the results. E.C. drafted the manuscript, and Z.Ü. reviewed and edited it. Both authors read and approved the final manuscript.

Funding No funding was received for this work.

Data availability The datasets generated and analysed during the current study are available from the corresponding author on reasonable request.

Declarations

Consent for publication Not applicable.

Competing interests The authors declare no competing interests.

Ethics approval Not applicable. The study used established cell lines only and involved no human participants or animals.

Consent to participate Not applicable.

Use of artificial intelligence tools An AI-based assistant was used to support threshold segmentation and counting of the archived Annexin V micrographs and to assist with language editing. All outputs were checked by the authors, who take full responsibility for the content of the manuscript.

References

1. Bray F, Laversanne M, Sung H, Ferlay J, Siegel RL, Soerjomataram I, Jemal A (2024) Global cancer statistics 2022: GLOBOCAN estimates of incidence and mortality worldwide for 36 cancers in 185 countries. CA Cancer J Clin 74:229–263. https://doi.org/10.3322/caac.21834
2. Dasari S, Tchounwou PB (2014) Cisplatin in cancer therapy: molecular mechanisms of action. Eur J Pharmacol 740:364–378. https://doi.org/10.1016/j.ejphar.2014.07.025
3. Ghosh S (2019) Cisplatin: the first metal based anticancer drug. Bioorg Chem 88:102925. https://doi.org/10.1016/j.bioorg.2019.102925
4. Galluzzi L, Senovilla L, Vitale I, Michels J, Martins I, Kepp O, Castedo M, Kroemer G (2012) Molecular mechanisms of

cisplatin resistance. Oncogene 31:1869–1883. https://doi.org/10.1038/onc.2011.384
5. Wang H, Luo Y, Qiao T, Wu Z, Huang Z (2018) Luteolin sensitizes the antitumor effect of cisplatin in drug-resistant ovarian cancer via induction of apoptosis and inhibition of cell migration and invasion. J Ovarian Res 11:93. https://doi.org/10.1186/s13048-018-0468-y
6. Huang JZ, Li LL, Tan XY, Wu ZY, Chen DW, Luo X (2022) The effect of calycosin-7-O-β-D-glucoside and its synergistic augmentation of cisplatin-induced apoptosis in SK-OV-3 cells. Curr Pharm Des 28:2161–2166. https://doi.org/10.2174/1381612828666220610164100
7. Jin Y, Wu Q, Pan S, Zhou Q, Liu H, Zhang Q, Zhang J, Zhu X (2024) Baicalein enhances cisplatin sensitivity in cervical cancer cells by promoting cuproptosis through the Akt pathway. Biomed Pharmacother 179:117415. https://doi.org/10.1016/j.biopha.2024.117415
8. Karimzadeh MR, Masoudi Chelegahi A, Shahbazi S, Reiisi S (2024) Co-treatment of silymarin and cisplatin inhibited cell proliferation, induced apoptosis in ovarian cancer. Mol Biol Rep 51:118. https://doi.org/10.1007/s11033-023-09026-8
9. Reed JC (1999) Dysregulation of apoptosis in cancer. J Clin Oncol 17:2941–2953. https://doi.org/10.1200/JCO.1999.17.9.2941
10. Oltvai ZN, Milliman CL, Korsmeyer SJ (1993) Bcl-2 heterodimerizes in vivo with a conserved homolog, Bax, that accelerates programmed cell death. Cell 74:609–619. https://doi.org/10.1016/0092-8674(93)90509-o
11. Peña-Blanco A, García-Sáez AJ (2018) Bax, Bak and beyond mitochondrial performance in apoptosis. FEBS J 285:416–431. https://doi.org/10.1111/febs.14186
12. Majeed NS, Salam AA, Farhan SR, Abdulrazzaq SA, Menon SV, Kaur M, Singh M, Husseen B, Jawad MA, Abedi-Firouzjah R (2025) Multifaceted roles of Bcl-2 family proteins: regulatory roles in apoptosis, physiological functions, and therapeutic potential. Curr Med Sci 45:1319–1335. https://doi.org/10.1007/s11596-025-00124-1
13. Imran M, Rauf A, Abu-Izneid T, Nadeem M, Shariati MA, Khan IA, Imran A, Orhan IE, Rizwan M, Atif M, Gondal TA, Mubarak MS (2019) Luteolin, a flavonoid, as an anticancer agent: a review. Biomed Pharmacother 112:108612. https://doi.org/10.1016/j.biopha.2019.108612
14. Park SH, Ham S, Kwon TH, Kim MS, Lee DH, Kang JW, Oh SR, Yoon DY (2014) Luteolin induces cell cycle arrest and apoptosis through extrinsic and intrinsic signaling pathways in MCF-7 breast cancer cells. J Environ Pathol Toxicol Oncol 33:219–231. https://doi.org/10.1615/jenvironpatholtoxicoloncol.2014010923
15. Magura J, Moodley R, Mackraj I (2022) The effect of hesperidin and luteolin isolated from Eriocephalus africanus on apoptosis, cell cycle and miRNA expression in MCF-7. J Biomol Struct Dyn 40:1791–1800. https://doi.org/10.1080/07391102.2020.1833757
16. Raina R, Pramodh S, Rais N, Haque S, Shafarin J, Bajbouj K, Hamad M, Hussain A (2021) Luteolin inhibits proliferation, triggers apoptosis and modulates Akt/mTOR and MAP kinase pathways in HeLa cells. Oncol Lett 21:192. https://doi.org/10.3892/ol.2021.12452
17. Zhao W, Liu J, Zhao S, Zheng J, Zhao J, Wang T, Wang M, Chen J, Tan W (2026) Effects and potential mechanisms of luteolin on cisplatin-mediated inhibition of cervical adenocarcinoma. Open Life Sci 21:20251274. https://doi.org/10.1515/biol-2025-1274
18. Chen YH, Wu JX, Yang SF, Hsiao YH (2023) Synergistic combination of luteolin and asiatic acid on cervical cancer in vitro and in vivo. Cancers (Basel) 15:548. https://doi.org/10.3390/cancers15020548
19. Seong SH, Yun B, Kim JH, Seo C, Han S, Kim TS, Kim BR, Lee HN, Im S, Kim JE, Jung JM, Choi KM, Jeong JW (2025) Herbacetin and gossypetin glycosides from Sedum kamtschaticum Fisch. & C. A. Mey. and S. takesimense Nakai, and their antioxidant, anti-aging, and monoamine oxidase inhibitory activities. Phytochemistry 242:114716. https://doi.org/10.1016/j.phytochem.2025.114716
20. Spiegel M, Kowalczyk A (2025) Aglycone, glycoside, or glucuronide? Experimental and mechanistic insights into the antioxidative potential of gossypetin, gossypin, and hibifolin. J Phys Chem B 129:7593–7601. https://doi.org/10.1021/acs.jpcb.5c03338
21. Huang K, Liu Z, Kim MO, Kim KR (2023) Anticancer effects of gossypetin from Hibiscus sabdariffa in oral squamous cell carcinoma. J Appl Oral Sci 31:e20230243. https://doi.org/10.1590/1678-7757-2023-0243
22. Xie X, Liu K, Liu F, Chen H, Wang X, Zu X, Ma X, Wang T, Wu Q, Zheng Y, Bode AM, Dong Z, Kim DJ (2018) Gossypetin is a novel MKK3 and MKK6 inhibitor that suppresses esophageal cancer growth in vitro and in vivo. Cancer Lett 442:126–136. https://doi.org/10.1016/j.canlet.2018.10.016
23. Lee MS, Tsai CW, Wang CP, Chen JH, Lin HH (2017) Anti-prostate cancer potential of gossypetin via inducing apoptotic and autophagic cell death. Mol Carcinog 56:2578–2592. https://doi.org/10.1002/mc.22702
24. Wang L, Zhang Z, Ge R, Zhang J, Liu W, Mou K, Lv S, Mu X (2019) Gossypetin inhibits solar-UV induced cutaneous basal cell carcinoma through direct inhibiting PBK/TOPK protein kinase. Anticancer Agents Med Chem 19:1029–1036. https://doi.org/10.2174/1871520619666190301123131
25. Kim H, Kim E, Ma L, Kim C, Park K, Liu Z, Huang K, Kim DJ, Ryoo ZY, Yi JK, Sung Y, Jang S, Kim MO (2025) Gossypetin alleviates DSS-induced colitis by regulating COX2 and ROS-JNK signaling. Curr Pharm Biotechnol 26:769–777. https://doi.org/10.2174/0113892010331882240901095733
26. Chen X, Wang Y, Li P, Yao J, Song Y, Jiang H, Zeng S, Chen L, Zhou H (2025) Quantification of gossypetin, myricetin, quercetin and isorhamnetin in mouse plasma: pharmacokinetic profiling after oral administration of total flavone of Abelmoschi Corolla. J Pharm Biomed Anal 265:117039. https://doi.org/10.1016/j.jpba.2025.117039
27. Da Rosa RB, Borsoi G, Conter LU, Feistel C, Gottems AL, Reginatto FH, Grivicich I, De Barros Falcão Ferraz A (2022) Bioguided isolation of a selective compound from Calea phyllolepis leaves against breast cancer cells. Basic Clin Pharmacol Toxicol 130:20–27. https://doi.org/10.1111/bcpt.13664
28. Mosmann T (1983) Rapid colorimetric assay for cellular growth and survival: application to proliferation and cytotoxicity assays. J Immunol Methods 65:55–63. https://doi.org/10.1016/0022-1759(83)90303-4
29. Vermes I, Haanen C, Steffens-Nakken H, Reutelingsperger C (1995) A novel assay for apoptosis. Flow cytometric detection of phosphatidylserine expression on early apoptotic cells using fluorescein labelled Annexin V. J Immunol Methods 184:39–51. https://doi.org/10.1016/0022-1759(95)00072-i
30. Zhang G, Gurtu V, Kain SR, Yan G (1997) Early detection of apoptosis using a fluorescent conjugate of annexin V. Biotechniques 23:525–531. https://doi.org/10.2144/97233pf01
31. Logue SE, Elgendy M, Martin SJ (2009) Expression, purification and use of recombinant annexin V for the detection of apoptotic cells. Nat Protoc 4:1383–1395. https://doi.org/10.1038/nprot.2009.143
32. Ghasemi A, Khanzadeh T, Zadi Heydarabad M, Khorrami A, Jahanban Esfahlan A, Ghavipanjeh S, Gholipour Belverdi M, Darvishani Fikouhi S, Darbin A, Najafpour M, Azimi A (2018) Evaluation of BAX and BCL-2 gene expression and apoptosis induction in acute lymphoblastic leukemia cell line CCRF-CEM after high-dose prednisolone treatment. Asian Pac J Cancer Prev 19:2319–2323. https://doi.org/10.22034/APJCP.2018.19.8.2319

33. Sulistiyowati I, Yunus J, Sari DCR, Arfian N (2020) Upregulation of p16, Bax and Bcl-2 mRNA expression associated with epithelial apoptosis and myofibroblast proliferation in kidney fibrosis model in mice. Malays J Med Sci 27:37–44. https://doi.org/10.21315/mjms2020.27.2.4
34. Livak KJ, Schmittgen TD (2001) Analysis of relative gene expression data using real-time quantitative PCR and the 2^–ΔΔCT method. Methods 25:402–408. https://doi.org/10.1006/meth.2001.1262
35. Bustin SA, van den Ruijter JM, Kubista M, Pfaffl MW, Shipley GL, Tran N, Rödiger S, Untergasser A, Mueller R, Nolan T, Milavec M, Burns MJ, Huggett JF, Vandesompele J, Wittwer CT (2025) MIQE 2.0: revision of the Minimum Information for Publication of Quantitative Real-Time PCR Experiments guidelines. Clin Chem 71:634–651. https://doi.org/10.1093/clinchem/hvaf043
36. Foucquier J, Guedj M (2015) Analysis of drug combinations: current methodological landscape. Pharmacol Res Perspect 3:e00149. https://doi.org/10.1002/prp2.149
37. Zhao W, Sachsenmeier K, Zhang L, Sult E, Hollingsworth RE, Yang H (2014) A new Bliss independence model to analyze drug combination data. J Biomol Screen 19:817–821. https://doi.org/10.1177/1087057114521867
38. Lin S, Chen Z, Li S, Chen B, Wu Y, Zheng Y, Huang J, Chen Y, Lin X, Yao H (2024) Anti-tumor effect and mechanism of the total biflavonoid extract from S. doederleinii on human cervical cancer cells in vitro and in vivo. Heliyon 10:e24778. https://doi.org/10.1016/j.heliyon.2024.e24778. Corrigendum: Heliyon 10:e30202. https://doi.org/10.1016/j.heliyon.2024.e30202
39. Özdemir İ, Afşin Y, Tuncer MC, Öztürk Ş (2025) Combined hesperidin and doxorubicin treatment induces apoptosis and modulates inflammatory cytokines in HeLa cervical cancer cells. Int J Mol Sci 26:8753. https://doi.org/10.3390/ijms26178753
40. International Organization for Standardization (2009) ISO 10993-5:2009 Biological evaluation of medical devices: Part 5: Tests for in vitro cytotoxicity. ISO, Geneva
41. Gruber S, Nickel A (2023) Toxic or not toxic? The specifications of the standard ISO 10993-5 are not explicit enough to yield comparable results in the cytotoxicity assessment of an identical medical device. Front Med Technol 5:1195529. https://doi.org/10.3389/fmedt.2023.1195529
42. Sezgin AK, Gündüz MK, Aydın E, Kaymak G (2026) Selective modulation of IL-6/JAK/STAT-related signaling under redox-shift conditions by luteolin. Mol Biol Rep 53:1088. https://doi.org/10.1007/s11033-026-12190-2
43. El Hajj J, Karam L, Jaber A, Cheble E, Akoury E, Kobeissy PH, Ibrahim JN, Yassin A (2024) Evaluation of antiproliferative potentials associated with the volatile compounds of Lantana camara flowers: selective in vitro activity. Molecules 29:5431. https://doi.org/10.3390/molecules29225431
44. n den Brand AD, Villevoye J, van den Nijmeijer SM, van Duursen MBM (2019) Anti-tumor properties of methoxylated analogues of resveratrol in malignant MCF-7 but not in non-tumorigenic MCF-10A mammary epithelial cell lines. Toxicology 422:35–43. https://doi.org/10.1016/j.tox.2019.04.009
45. Alkan Akalın S, Afşin Y, Özdemir İ, Tuncer MC, Öztürk Ş (2025) Integrated molecular analysis of thymoquinone–methotrexate synergy in breast cancer cells: apoptosis, oxidative stress, and pathway modulation. Pharmaceuticals (Basel) 18:1551. https://doi.org/10.3390/ph18101551
46. Faal MA, Tasbandi T, Aliyari M, Shojaei M, Eskandari M, Sahebkar A, Hosseini H, Jalili-Nik M (2026) Synergistic effects of Calebin A and docetaxel on apoptosis and migration in prostate cancer cells. Daru 34:3. https://doi.org/10.1007/s40199-025-00579-6
47. ter Riet G, Korevaar DA, Leenaars M, Sterk PJ, Van Noorden CJF, Bouter LM, Lutter R, Oude Elferink RP, Hooft L (2012) Publication bias in laboratory animal research: a survey on magnitude, drivers, consequences and potential solutions. PLoS ONE 7:e43404. https://doi.org/10.1371/journal.pone.0043404
48. Bruggisser R, von Daeniken K, Jundt G, Schaffner W, Tullberg-Reinert H (2002) Interference of plant extracts, phytoestrogens and antioxidants with the MTT tetrazolium assay. Planta Med 68:445–448. https://doi.org/10.1055/s-2002-32073
49. Peng L, Wang B, Ren P (2005) Reduction of MTT by flavonoids in the absence of cells. Colloids Surf B Biointerfaces 45:108–111. https://doi.org/10.1016/j.colsurfb.2005.07.014

Publisher's note Springer Nature remains neutral with regard to jurisdictional claims in published maps and institutional affiliations.

Springer Nature or its licensor (e.g. a society or other partner) holds exclusive rights to this article under a publishing agreement with the author(s) or other rightsholder(s); author self-archiving of the accepted manuscript version of this article is solely governed by the terms of such publishing agreement and applicable law.